Reorganization of circuits underlying cerebellar modulation of prefrontal cortical dopamine in mouse models of autism spectrum disorder

Tiffany D. Rogers[1], **Price E. Dickson**[1], **Eric McKimm**[1], **Detlef H. Heck**[2], **Dan Goldowitz**[3], **Charles D. Blaha**[1,*], and **Guy Mittleman**[1]

[1]Department of Psychology, University of Memphis, Memphis, TN 38152, USA

[2]Department of Anatomy & Neurobiology, University of Tennessee Health Science Center, Memphis, TN 38163, USA

[3]Centre for Molecular Medicine & Therapeutics, Department of Medical Genetics, University of British Columbia, Vancouver, BC V5Z 4H4, Canada

Abstract

Imaging, clinical and pre-clinical studies have provided ample evidence for a cerebellar involvement in cognitive brain function including cognitive brain disorders, such as autism and schizophrenia. We previously reported that cerebellar activity modulates dopamine release in the mouse medial prefrontal cortex (mPFC) via two distinct pathways: (1) cerebellum to mPFC via dopaminergic projections from the ventral tegmental area [VTA] and (2) cerebellum to mPFC via glutamatergic projections from the mediodorsal and ventrolateral thalamus (ThN md and vl). The present study compared functional adaptations of cerebello-cortical circuitry following developmental cerebellar pathology in a mouse model of developmental loss of Purkinje cells (*Lurcher*) and a mouse model of fragile X syndrome (*Fmr1* KO mice). Fixed potential amperometry was used to measure mPFC dopamine release in response to cerebellar electrical stimulation. Mutant mice of both strains showed an attenuation in cerebellar-evoked mPFC dopamine release compared to respective wildtype mice. This was accompanied by a functional reorganization of the VTA and thalamic pathways mediating cerebellar modulation of mPFC dopamine release. Inactivation of the VTA pathway by intra-VTA lidocaine or kynurenate infusions decreased dopamine release by 50% in wildtype and 20-30% in mutant mice of both strains. Intra-ThN vl infusions of either drug decreased dopamine release by 15% in wildtype and 40% in mutant mice of both strains, while dopamine release remained relatively unchanged following intra-ThN md drug infusions. These results indicate a shift in strength towards the thalamic vl projection, away from the VTA. Thus, cerebellar neuropathologies associated with autism spectrum disorders may cause a reduction in cerebellar modulation of mPFC dopamine release that is related to a reorganization of the mediating neuronal pathways.

Keywords

Autism Spectrum Disorders; cerebellum; prefrontal cortex; dopamine; Fragile X; Lurcher

---

*Correspondence to: Dr. Charles D. Blaha Department of Psychology The University of Memphis Memphis, Tennessee, USA 38152-6400, cblaha@memphis.edu.

Introduction

Autism is a neurodevelopmental disorder characterized by deficits in social skills and communication, unusual and repetitive behavior, and deficits in cognitive function [1]. Neuropsychological testing has revealed that patients with autism also have specific deficits in cognitive function including impairments in memory and attention, executive function, planning, cognitive flexibility, rule acquisition, and abstract thinking [2]. The etiological factors in autism and autism spectrum disorders (ASD) are enigmatic and have been linked to genetic mutations as well as exposure to environmental agents [3-7].

Regardless of etiology, cerebellar neuropathology commonly occurs in autistic individuals. Cerebellar hypoplasia and reduced cerebellar Purkinje cell numbers are the most consistent neuropathologies linked to autism [8-13]. MRI studies report that autistic children have smaller cerebellar vermal volume in comparison to typically developing children [14]. Postmortem studies indicate that in addition to reduced Purkinje cell numbers, microanatomic abnormalities of the cerebellum in this population include excess Bergmann glia, reductions in the size and number of cells in the deep cerebellar nuclei, and an active neuroinflammatory process within cerebellar white matter [15-17].

Using a mouse model we have previously investigated how developmental damage of the cerebellum influences the appearance of autism-like symptoms and cognitive deficits, as well as the neural mechanisms by which this could occur. *Lurcher* (*Lc*/+) mutant mice have an autosomal dominant mutation that results in a nearly complete loss of cerebellar Purkinje cells between the 2nd and 4th weeks of life [18, 19]. Since these mice are ataxic we have used non-ataxic chimeric mice (*Lc*/+↔+/+), which have a variable loss of Purkinje cells dependent upon the incorporation of the wildtype lineage, to examine the behavioral impact of cerebellar Purkinje cell loss [20]. We found that: (1) Chimeric mice with reduced numbers of cerebellar Purkinje cells show exaggerated repetitive behaviors [21]. (2) *Lurcher* mice and chimeras display impaired executive function as measured in a serial reversal learning task [22]. (3) Both repetitive behaviors and executive function errors were significantly, negatively correlated with the number of Purkinje cells obtained from cell counts [21, 22]. (4) Cerebellar output through the dentate nucleus (DN) modulates dopamine release in the medial prefrontal cortex (mPFC) via two independent pathways [23]. Both of these pathways originate in the cerebellar cortex and then project to the deep cerebellar nuclei (see inset in Fig. 3). The first involves indirect activation of mesocortical dopaminergic neurons via contralateral glutamatergic projections of the DN to reticulo-tegmental nuclei (RTN) that, in turn, project to pedunculopontine nuclei (PPT) and then project to, and stimulate directly, ventral tegmental area (VTA) dopaminergic cell bodies projecting to the medial mPFC [24-28]. The second involves activation of the contralateral glutamatergic projections of the DN to thalamic mediodorsal and ventrolateral nuclei (ThN md and ThN vl) that send glutamatergic efferents to the mPFC to modulate mesocortical dopaminergic terminal release in the mPFC via appositional excitatory glutamatergic synapses [29-31]. (5) Blocking glutamatergic transmission along either of these pathways reduced cerebellar dependent mPFC dopamine release by around 50% in each case, suggesting that the two pathways contribute equally and that they are primarily, if not entirely, glutamatergic [32]. Dopamine dysregulation in the mPFC is thus a possible neuronal mechanism underlying the deficits in repetitive behaviors and executive function [22].

The aim of the present study was to compare adaptations of cerebello-cortical circuitry mediating cerebellar mPFC dopamine modulation following developmental cerebellar pathology relevant to ASD. We used two mutant mouse strains with different forms of cerebellar deficits.

Fragile X syndrome is one of the rare ASD with a known monogenetic cause, here the loss of function of the *Fmr1* gene. *Fmr1*-KO mice have an *Fmr1*$^{\text{tm1Cgr}}$ targeted mutation and are widely used as a mouse model of fragile X syndrome [33, 34]. *Fmr1*-KO mice display cerebellar abnormalities such as elongated Purkinje cell spines and decreased volume of deep cerebellar nuclei [35, 36]. Mice from the second mutant strain used here (*Lurcher*) suffer from developmental loss of all cerebellar Purkinje cells. There is no known human equivalent to this genetic condition. We used fixed potential amperometry to monitor mPFC dopamine release evoked by DN electrical stimulation before and after inactivation of glutamatergic transmission through the ThN md/ThN vl and VTA pathways in urethane anesthetized mice.

Materials and methods

Animals

Experimental subjects were bred and maintained in the Animal Care Facility located in the Department of Psychology at the University of Memphis. Mice were continuously maintained in a temperature controlled environment ($21 \pm 1°C$) on a 12:12 light:dark cycle (lights on at 0800) and were given free access to food and water. Original *Lurcher* (#001046) and *Fmr1* breeders (#004624, #004828) were purchased from The Jackson Laboratory (Bar Harbor, Maine). All experiments were approved by a local Institutional Animal Care and Use Committee and conducted in accordance with the National Institutes of Health Guidelines for the Care and Use of Laboratory Animals.

Breeding

To produce *Lurcher* mutant mice, ataxic male mice heterozygous for the *Lurcher* spontaneous mutation (B6CBACa A^{w-J}/A-Grid2^{Lc}) were bred with non-ataxic female wildtype mice (B6CBACa A^{w-J}/A-Grid2$^+$). This breeding strategy produced litters composed of both heterozygous mutant and wildtype mice. Due to their ataxic gait, mice heterozygous for the *Lurcher* mutation are easily distinguishable from their non-ataxic wildtype littermates.

Two phases of breeding were required to produce *Fmr1* KO mice. In the first phase, male mice hemizygous for the *Fmr1*^{tm1Cgr} targeted mutation (FVB.129P2-*Fmr1*^{tm1Cgr}/J) were bred with female wildtype mice (FVB.129P2-*Pde6b*$^+$*Tyr*$^{c-ch}$/AntJ). This breeding strategy produced litters composed only of heterozygous females and wildtype males. In the second phase, heterozygous female mice were bred with wildtype male mice to produce litters containing both hemizygous and wildtype males which were subsequently used as experimental subjects. Genotyping of all *Fmr1* mice used in present study was performed by Transnetyx (Cordova, TN).

Surgery

Mice were anaesthetized with urethane (1.5g/kg, i.p.) and placed in a stereotaxic frame with head-holder adaptor. Body temperature was maintained at $36 \pm 0.5°$ C with a temperature-regulated heating pad. Four holes were drilled into the animals' skulls to allow for the implantation of an Ag/AgCl reference/auxiliary combination electrode, a carbon-fiber microelectrode (dopamine recording electrode; carbon fiber 10 μm o.d., 250 μm length, Thornel Type P, Union Carbide, PA; [24]), a concentric bipolar stimulating electrode (CBARD75, 125 μm outer and 25 μm inner pole diam., FHC, ME), and a 31g stainless-steel guide cannula for drug microinfusions into appropriate nuclei. The Ag/AgCl reference/auxiliary combination electrode was placed at the surface of the cortex and contralateral to the recording electrode which was placed in mPFC of the left hemisphere at a 30° lateral to medial angle (coordinates from bregma: AP +2.35 mm, ML +1.0 mm, DV -1.5 mm from

dura; [37]). The stimulating electrode was placed in the right DN (coordinates from bregma: AP -6.24 mm, ML -2.1 mm, DV -2.25 mm from dura [37]). Due to differences in cerebellum size from the developmental loss of Purkinje cells and based on histological analysis the stimulating electrode [23] coordinates for the right DN in Lurcher mutant mice corresponded to: (from bregma: AP -5.85 mm, ML -1.0 mm, DV -1.0 mm from dura). The guide cannula tip was placed 1 mm above in the VTA, ThN md, or ThN vl (coordinates from bregma: AP -3.3 mm, ML +0.35 mm, DV -3.0 mm from dura; AP -1.35 mm, ML +0.4 mm, DV -2.75 mm from dura; AP -1.35 mm, ML +1.0 mm, DV -3.45 mm from dura, respectively [37]).

Fixed potential amperometry and electrical stimulations

After implantation of all electrodes and cannulae, a constant voltage of +0.8 V was applied to the recording electrode and oxidation current (corresponding to changes in extracellular dopamine concentrations) sampled continuously (10,000 samples/sec) via an electrometer (ED401 e-corder 401 and EA162 Picostat, eDAQ Inc., CO, USA) filtered at 10 Hz low pass [24]. Electrical stimulation of the DN consisted of 100 cathodic monophasic pulses (400 μA intensity, 0.5 ms pulse duration) at 50 Hz every 60 seconds for a period of 10 to 15 minutes and were applied to the stimulating electrode via an optical isolator and programmable pulse generator (Iso-Flex/Master-8; AMPI, Jerusalem, Israel).

Pathway inactivations

Following approximately 5 minutes of baseline recording, separate groups of mice received microinfusions of lidocaine (0.02 μg), kynurenate (0.5 μg), or 10 mM phosphate-buffered saline (PBS). Infusions were administered via the guide cannula. Drugs were first back-loaded into a fiberglass infusion cannula (80 μm o.d., Polymicro Tech. Inc., AZ, USA) and then connected via PE10 tubing to a 1.0 μl microsyringe (Scientific Glass Engineering, Inc., TX, USA). The infusion cannula was then placed into the guide cannula to extend 1 mm from its tip into the injection site. A 0.5 μl infusion of lidocaine, kynurenate, or PBS was then administered over a 1.0 min period and left in place for an additional minute. Changes in DN stimulation-evoked dopamine oxidation current in the mPFC were then recorded for 10 minutes post-infusion.

Data analyses

The three DN stimulation-evoked responses immediately prior to each drug infusion as well as the three responses following infusion were extracted from the continuous record and amperometric currents within the range of 0.2s pre-stimulation and 60s post-stimulation were normalized to zero current values. The currents for each evoked response were then summed across time (-0.2s through 60s) for each response due to dopamine concentrations significantly differing from pre-stimulation baseline for several seconds post-stimulation [23, 32]. As the pre-infusion responses and the post-infusion responses were each one minute apart, two repeated measures analyses of variance (ANOVA) were conducted for each mouse genotype with time (1-3) of each pre-infusion response or time (1-3) of each post-infusion response, as a within-groups factor. For all analyses, Site of infusion and Drug administered were between-group factors and the response sums at each time point were the dependent variable. These analyses indicated that the stimulation-evoked responses did not differ significantly across either pre-infusion times (1-3) or post-infusion times (1-3) (p > .05). Because the stimulation-evoked responses did not vary significantly, we averaged the three pre- and post- infusion response current sum values to determine pre- with post-infusion responses, respectively. Effects of infusion for each mouse were expressed as average post-infusion changes relative to pre-infusion baseline responses.

Using average post infusion percent decrease as the dependent variable, the general data analytic strategy was analysis of variance (ANOVA). Depending on the ANOVA, Strain (*Lurcher* or *Fmr1*), Genotype (wildtype or mutant), Site (VTA, ThN md, or ThN vl) and Drug (PBS, lidocaine or kynurenate) were used as the between subjects factors. Interactions were investigated with either Sidak-Bonferroni post-hoc comparisons or simple main effects tests.

Histology

Immediately following each experiment, a direct current (100 μA for 10 s; +5 V for 5 sec) was passed through the stimulating electrode in the DN to leave iron deposits and through the recording electrode in the mPFC to lesion tissue, respectively. Each mouse was then euthanized with a lethal intracardial injection of urethane. The brains were removed and preserved overnight in 10% buffered formalin containing 0.1% potassium ferricyanide, and then stored in 30% sucrose/10% formalin solution until sectioning. At the conclusion of the experiment, the brains were sectioned on a cryostat at -30° C. A Prussian blue spot indicative of the redox reaction of ferricyanide and iron deposits labeled the stimulating electrode tip in the DN, while placements of the recording electrodes in the mPFC were determined by the position of the electrolytic lesion and placements of cannulas were determined by the position of the drug infusion guide cannula. Placements of the electrodes and cannulae were confirmed under light microscopy and recorded on representative coronal diagrams [37].

Results

Stereotaxic placements of electrodes and drug infusion cannulae

Figure 1 depicts the central placements of stimulating and recording electrodes and infusion cannula tips in each mouse genotype. In *Lurcher* mutants (n = 54) the stimulating electrode tip locations were confined within the DN ranging from, in mm, -5.4 to -6.2 AP, +0.7 to +1.3 ML, and -0.7 to -1.4 DV In all other groups, the stimulating electrode tip locations were confined within the DN (n = 135 electrodes, ranging from, in mm, -6.0 to -6.5 AP, +1.7 to +2.7 ML, and -2.1 to -3.25 DV) posterior to bregma, lateral to midline, and ventral from dura. Infusion cannula tips were confined to the ThN md (n = 63; ranging from in mm: -1.05 to -1.45 AP, +0.15 to +0.7 ML, and -2.4 to -3.5 DV), the ThN vl (n =63; ranging from in mm, -1.2 to -1.45 AP, +0.6 to +1.3 ML, and -3.1 to -3.95 DV), and the VTA (n = 63; ranging from in mm: -3.1 to -3.3 AP, +0.15 to +0.55 ML, and -3.6 to -4.5 DV) posterior to bregma, lateral to midline, and ventral from dura. Recording electrode surface locations were confined within the mPFC (n = 189; ranging from in mm: +2.2 to +2.6 AP, +0.1 to +0.6 ML, and -0.8 to -1.55 DV) anterior to bregma, lateral to midline and ventral from dura.

Drug pre-infusion DN stimulation-evoked dopamine release

Figure 2 shows representative mPFC dopamine release evoked by DN stimulation, immediately prior to drug infusion. Regardless of mouse strain or genotype, electrical stimulation (100 pulses at 50 Hz) of the DN evoked a significant increase in mPFC dopamine release (change in oxidation current) that peaked within 5 seconds after stimulation and then declined gradually towards baseline pre-stimulation levels over the course of approximately 1 min. The time course of DN stimulation-evoked mPFC dopamine release was similar in both mutant and wildtype mice of both strains. However, mutants of both strains showed a marked and consistent attenuation in the magnitude of evoked dopamine release compared to their wildtype littermates.

Effects of drug infusions on DN stimulation-evoked dopamine release in mPFC

An initial ANOVA used Strain (*Lurcher* or *Fmr1*), Genotype (wildtype or mutant), Site of infusion (VTA, ThN md, or ThN vl) and Drug (PBS, lidocaine, or kynurenate) as factors. This analysis indicated that mouse Strain interacted significantly with Genotype and Site of infusion ($F(2,153) = 4.5$, $p=.01$), and that mouse Genotype interacted significantly with Site and Drug ($F(4,153) = 32.22$, $p < .001$). Thus, subsequent ANOVAs were used to compare wildtype and mutant animals within either the *Lurcher* or *Fmr1* strains. These ANOVAs again indicated that wildtype and mutant mice within each strain differed significantly as a function of Drug and Site of infusion (*Lurcher*: $F(4,81) = 10.20$, $p<.001$; *Fmr1*: $F(4,72) = 38.76$, $p<.001$). Therefore a third series of four ANOVAs was conducted on each genotype (*Lurcher* wildtype, *Lurcher* mutant, *Fmr1* wildtype and *Fmr1* mutant mice).

Table 1 shows the infusion site-specific percent decreases following PBS, lidocaine, or kynurenate in each mouse strain. Both lidocaine and kynurenate infusions at each of the injection sites achieved their maximal inhibitory effects on DN stimulation-evoked dopamine release in the mPFC within 1 min of infusion. ANOVAs indicated a significant interaction between Drug and Site of infusion for each mouse genotype (*Lurcher* wildtype mice: $F(4, 36) = 467.51$, $p=.001$; *Lurcher* mutant mice: $F(4, 45) = 4.261$, $p = .005$; *Fmr1* wildtype mice: $F(4, 36) = 34.78$, $p < .001$; *Fmr1* mutant mice: $F(4, 36) = 12.79$, $p < .001$). Sidak-Bonferroni post-hoc comparisons indicated that the average percent decrease in DN stimulation-evoked mPFC dopamine release in all groups receiving PBS was significantly different from that of the associated groups receiving either lidocaine or kynurenate ($p < .008$). Additionally, the average percent decrease in DN stimulation-evoked mPFC dopamine release of each group receiving lidocaine did not differ significantly from that of the groups of the same mouse genotype which received kynurenate ($p >.05$).

As the average percent decrease of DN stimulation-evoked mPFC dopamine release was similar following either lidocaine or kynurenate, simple main effects tests were conducted on the kynurenate results in order to determine significant differences between wildtype and mutant animals following drug infusion into VTA, ThN md, or ThN vl. By comparing kynurenate-induced attenuation in wildtype and mutant mice within the same strain, it was possible to determine the relative contributions of pathways through the VTA, ThN md, or ThN vl to total DN stimulation-evoked mPFC dopamine release. As shown in figure 3, dopamine release declined by ∼50% following VTA infusion of kynurenate in *Lurcher* wildtype mice, which indicated that this pathway accounted for 50% of the total DN stimulation-evoked mPFC dopamine release. In contrast, there was an attenuation of only ∼30% in *Lurcher* mutants, indicating a 20% reduction in dopamine modulatory strength in the pathway through the VTA. This difference between *Lurcher* wildtype and mutant mice was significant ($F(1,9) = 10.86$, $p = .009$). Very similar results were obtained in *Fmr1* wildtype (∼50% decrease) and mutant (∼20% decrease) mice following infusion of kynurenate into the VTA ($F(1,8) = 279.38$, $p < .001$).

Kynurenate-induced reductions in DN stimulation-evoked mPFC dopamine release following infusions into the ThN md ranged between ∼30 to 40% in wildtype and mutant mice of both strains. Wildtype and mutant mice of the *Lurcher* ($F(1,9) = 1.47$, $p=ns$) or *Fmr1* ($F(1, 8) = 1.86$, $p=ns$) strains did not differ significantly in the response to intra-ThN md kynurenate infusions.

Following kynurenate infusion into the ThN vl, DN stimulation-evoked mPFC dopamine release was reduced by ∼15% in both *Lurcher* and *Fmr1* wildtype mice. In marked contrast, evoked mPFC dopamine release in *Lurcher* and *Fmr1* mutant mice decreased by ∼40%. In both strains the mutant and wildtype mice differed significantly following kynurenate infusion into the ThN vl (*Lurcher*: $F(1,9) = 61.02$, $p<.001$; *Fmr1*: $F(1, 8) = 313.70$, $p<.001$).

Considered together with the effects of kynurenate in the VTA these results indicate that the *Lc/+* and *Fmr1* mutations were associated with a decrease in dopamine modulatory strength in the DN → RTN → PPT → VTA → mPFC pathway along with a compensatory increase in strength in the DN → ThN vl → mPFC pathway. Dopamine modulation strength through the ThN md pathway was similar regardless of strain or genotype. It should be noted that within each mouse genotype the sum of the percent decreases for both pathways accounted for 100% of stimulation-evoked dopamine release recorded in the mPFC. It is thus unlikely that a third alternative pathway exists that was not investigated here.

Discussion

Developmental neuropathology of the cerebellum is a common occurrence in autism and ASD. The current study aimed to compare changes in cerebello-cortical circuitry mediating cerebellar modulation of mPFC dopamine in two strains of mutant mice with cerebellar neuropathology associated with ASD. Our results confirm previous findings of two separate, glutamatergic pathways, the VTA (DN → RTN → PPT → VTA → mPFC) and the thalamic (DN → ThN md/vl → mPFC) pathway for cerebellar modulation of mPFC dopamine [23, 32]. The average percent decrease in DN stimulation-evoked mPFC dopamine release following infusion of the sodium channel blocker lidocaine or the broadspectrum glutamate receptor antagonist kynurenate into the VTA, ThN md, or ThN vl did not significantly differ, confirming that both pathways are primarily glutamatergic. Additionally, because mPFC dopamine release reductions following inactivation of the thalamic and VTA pathways summed to ~100%, cerebellar modulation of mPFC dopamine appears to be completely accounted for by these two pathways.

Here we show that cerebellar neuropathology is associated with weakening of cerebellar modulation of mPFC dopamine transmission (see Fig. 2) and with a functional reorganization of the balance between the two pathways (see Fig. 3). In wildtype mice of both strains, cerebellar modulation of mPFC dopamine was mediated equally by the VTA and thalamic pathways. However, in both the *Lurcher* mutant and *Fmr1* mutants, there was a shift in modulatory control away from the VTA towards the thalamic pathway, with a specific increase in modulatory strength on the dopamine signal through the ThN vl.

It seems reasonable that this shift away from the VTA may be the result of a loss of cerebellar output as both *Lurcher* and *Fmr1* mutant mice have been reported to have cerebellar abnormalities that could impair cerebello-cortical connectivity. As noted previously *Lurchers* loose nearly all Purkinje cells, which constitute the sole output of the cerebellar cortex [18, 19], but maintain most of their cerebellar nuclei, the main cerebellar output structure, but with abnormally potentiated GABAergic conductances [38]. *Fmr1* mutant mice are reported to have more subtle cerebellar neuropathology including elongated spines on cerebellar Purkinje cells and decreased volume of deep cerebellar nuclei, which may also be indicative of reduced cerebellar output [35. 36]. Despite having different cerebellar abnormalities, both the *Lurcher* and *Fmr1* mutant mice display similar adaptations of cerebello-mPFC dopamine modulating circuitry with overall modulatory control weakened and a shift in balance from the VTA to the thalamic circuit. These similarities in adaptation are also noteworthy given the different genetic backgrounds of *Lurcher* (BL6) and *Fmr1* mice (FVB).

We suggest that the observed reorganization of cerebello-cortical circuitry as well as the attenuation of modulatory influence may underlie the cognitive deficits previously observed in *Lurcher* mice and *Lurcher*-WT chimeras, in that both the frequency of stereotyped repetitive behavior and the severity of deficits in executive function were specifically correlated with cerebellar Purkinje cell number [21, 23]. While relationships between

cerebellar neuropathology and cognitive deficits in *Fmr1* mutants have not been specifically investigated, it remains possible that some cognitive deficits including hyperactivity and increased perseveration could be linked to the observed reorganization of cerebello-cortical circuitry as the mPFC plays a role in both deficits [39-42].

Converging evidence from clinical studies increasingly supports the notion that developmental cerebellar neuropathology is associated with autism and ASD. Our data link cerebellar neuropathology directly to deficits in mPFC dopamine regulation through developmental adaptive changes in cerebello-cortical circuitry. Relevant to ASD, cerebellar abnormalities such as ectopic Purkinje cells, focal cerebellar Purkinje cell loss, and Bergmann gliosis are associated with Fragile X syndrome [43, 44]. Asperger's syndrome has been associated with lower total cerebellar volume and lower gray matter volume in the right cerebellum [45-47]. According to postmortem studies, patients with Rett syndrome display reduced volume of the cerebellum, cerebellar atrophy, and reduced Purkinje cell number [48, 49].

Indirect evidence of changes in cerebello-cortical circuitry comes from a variety of sources. Prefrontal cortex and thalamic abnormalities are found in patients with autism and the degree of abnormality in these areas is correlated with severity of symptoms. Our data suggest that these deficits might, at least in part, be caused by deficiencies in cerebellar output affecting cerbello-cortical pathways. During early brain development, the frontal cortex is larger in individuals with autism, and increased volume of frontal lobe cortex has been shown to be positively correlated with autistic symptoms [50, 51]. Importantly, the degree of enlargement of the frontal cortex is also positively correlated with the degree of hypoplasia in the cerebellum [52]. While total brain volume is positively correlated with the volume of the thalamus in control brains, a lack of correlation exists between total brain volume and volume of the thalamus in autistic brains [53-55]. The size of the thalamus in autistic patients is reduced when compared to controls, and the size of the left thalamus in children with ASD is inversely correlated with stereotypical and repetitive behaviors [54, 56].

Thus far, dopamine activity in the mPFC has received little attention in connection with ASD. A single pre-clinical study indicated dopaminergic abnormalities in the mPFC of autistic children. Using positron emission tomography (PET) it was found that autistic children have reduced dopaminergic activity in the mPFC compared to controls [57]. Lower levels of mPFC dopamine activity have been associated with deficits to a variety of cognitive functions including attention, working memory, and planning [58-61].

While evidence from patients and from mouse models of autism suggests that the cerebellar pathology associated with autism results in adaptations in cerebello-cortical circuitry and cognitive deficits, it is unclear whether these neuropathologies occur as part of the cascade of events that follow developmental cerebellar damage, or how they contribute to the range of symptom severity commonly observed in autism and ASD. It should be noted that a diverse range of abnormalities in other brain areas have been reported in *Lurcher* and *Fmr1* mutant mice. *Lurcher* mutant mice display prominent ataxia and are impaired in motor-related learning tasks. Given that the PPT also projects to dopaminergic neurons in the substantia nigra [24], it is conceivable that nigrostriatal dopaminergic transmission may be disrupted in *Lurcher* and possibly *Fmr1* mutant mice. However, there appear to be no differences in striatal tissue content of dopamine and its metabolites or in the densities of dopamine reuptake sites and D1 and D2 receptors in *Lurcher* mutant and wildtype mice (62-64). Regardless, autism patients also display neuropathologies in multiple brain areas in addition to the cerebellum. While the striking similarities observed in the adaptation of cerebello-mPFC dopamine mediating circuitry in the two mouse models support the notion

that they are due to shared cerebellar deficits, additional studies involving exclusive cerebellar pathology are required to confirm our notion (e.g., conditional KOs directed specifically to Purkinje or granule cells).

Conclusions

We have previously shown that the cerebellum modulates mPFC dopamine release via two distinct glutamatergic pathways [23, 32]. Here we show that developmental cerebellar pathology associated with ASD causes a reorganization of cerebello-cortical circuitry which results in attenuated modulation of mPFC dopamine transmission and a shifting of balance between the two pathways. Our results suggest that these functional modifications in cerebello-cortical connectivity may be a common consequence of developmental damage to the cerebellum with potential relevance to cerebellar cognitive function in general.

Acknowledgments

References

1. American Psychiatric Association. Diagnostic and Statistical Manual of Mental Disorders-IV-TR. 4th. Washington, DC: American Psychiatric Association; 2000.

2. Ozonoff, S.; South, M.; Provencal, S. Executive functions in autism: Theory and practice. In: Pérez, JM.; González, PM.; Comí, MC., et al., editors. New Developments in Autism: The Future is Today. Philadelphia: Asociación de Padres de Personas con Autismo; 2007. p. 185-213.

3. Bandim JM, Ventura LO, Miller MT, Almeida HC, Costa AES. Autism and Möbius sequence: An exploratory study of children in northeastern Brazil. Arq Neuropsiquiatr. 2003; 61:181–185. [PubMed: 12806493]

4. Devlin B, Scherer SW. Genetic architecture in autism spectrum disorder. Curr Opin Genet Dev. 2012; 22:229–37. [PubMed: 22463983]

5. Moore SJ, Turnpenny P, Quinn A, Glover S, Lloyd DJ, Montgomery T, Dean JC. A clinical study of 57 children with fetal anticonvulsant syndromes. J Med Genet. 2000; 37:489–497. [PubMed: 10882750]

6. Muhle R, Trentacoste SV, Rapin I. The genetics of autism. Pediatrics. 2004; 113:472–486.

7. Rodier PM. Converging evidence for brain stem injury in autism. Dev Psychopathol. 2002; 14:537–557. [PubMed: 12349873]

8. Bauman ML. Microscopic neuroanatomic abnormalities in autism. Pediatrics. 1991; 87:791–796. [PubMed: 2020538]

9. Courchesne E. Brainstem, cerebellar and limbic neuroanatomical abnormalities in autism. Current Opinion in Neurobiology. 1997; 7:269–278. [PubMed: 9142760]

10. Courchesne E, Townsend J, Akshoomoff NA, Saitoh O, Yeung-Courchesne R, Lincoln AJ, Lau L. Impairment in shifting attention in autistic and cerebellar patients. Behavioral Neuroscience. 1994; 108:848–865. [PubMed: 7826509]

11. Courchesne E, Yeung-Courchesne R, Press GA, Hesselink JR, Jernigan TL. Hypoplasia of cerebellar vermal lobules VI and VII in autism. New England Journal of Medicine. 1988; 318:1349–1354. [PubMed: 3367935]

12. DiCicco-Bloom E, Lord C, Zwaigenbaum L, Courchesne E, Dager SR, Schmitz C, Young LJ. The developmental neurobiology of autism spectrum disorder. Journal of Neuroscience. 2006; 26:6897–6906. [PubMed: 16807320]

13. Palmen SJ, van Engeland H, Hof PR, Schmitz C. Neuropathological findings in autism. Brain. 2004; 127:2572–2583. [PubMed: 15329353]

14. Webb SJ, Sparks BF, Friedman SD, Shaw DW, Giedd J, Dawson G, Dager SR. Cerebellar vermal volumes and behavioral correlates in children with autism spectrum disorder. Psychiatry Res. 2009; 172:61–67. [PubMed: 19243924]

15. Bauman ML, Kemper TL. Neuroanatomic observations of the brain in autism: A review and future directions. International Journal of Developmental Neuroscience. 2005; 23:183–187. [PubMed: 15749244]

16. Bailey A, Luthert P, Dean A, Harding B, Janota I, Montgomery M, Lantos P. A clinicopathological study of autism. Brain. 1998; 121:889–905. [PubMed: 9619192]

17. Vargas DL, Nascimbene C, Krishnan C, Zimmerman AW, Pardo CA. Neuroglial activation and neuroinflammation in the brain of patients with autism. Ann Neurol. 2005; 57:67–81. [PubMed: 15546155]

18. Caddy KW, Biscoe TJ. Structural and quantitative studies on the normal C3H and Lurcher mutant mouse. Philosophical transactions of the Royal Society of London. 1979; 287:167–201. [PubMed: 41272]

19. Zuo J, De Jager PL, Takahashi KA, Jiang W, Linden DJ, Heintz N. Neurodegeneration in Lurcher mice caused by mutation in delta2 glutamate receptor gene. Nature. 1997; 388:769–773. [PubMed: 9285588]

20. Goldowitz, D.; Moran, H.; Wetts, R. Mouse chimeras in the study of genetic and structural determinants of behavior. In: Goldowitz, D.; Wahlsten, D.; Wimer, RE., editors. Techniques for the Genetic Analysis of Brain and Behavior: Focus on the Mouse. Amsterdam: Elsevier; 1992. p. 271-290.

21. Martin LA, Goldowitz D, Mittleman G. Repetitive behavior and increased activity in mice with Purkinje cell loss: a model for understanding the role of cerebellar pathology in autism. European Journal of Neuroscience. 2010; 31:544–555. [PubMed: 20105240]

22. Dickson PE, Rogers TD, Del Mar N, Martin LA, Heck D, Blaha CD, Mittleman G. Behavioral flexibility in a mouse model of developmental cerebellar Purkinje cell loss. Neurobiology of Learning and Memory. 2010; 94:220–228. [PubMed: 20566377]

23. Mittleman G, Goldowitz D, Heck DH, Blaha CD. Cerebellar modulation of frontal cortex dopamine efflux in mice: Relevance to autism and schizophrenia. Synapse. 2008; 62:544–550. [PubMed: 18435424]

24. Forster GL, Blaha CD. Pedunculopontine tegmental stimulation evokes striatal dopamine efflux by activation of acetylcholine and glutamate receptors in the midbrain and pons of the rat. European Journal of Neuroscience. 2003; 17:751–762. [PubMed: 12603265]

25. Garcia-Rill E, Skinner RD, Miyazato H, Homma Y. Pedunculopontine stimulation induces prolonged activation of pontine reticular neurons. Neuroscience. 2001; 104:455–465. [PubMed: 11377847]

26. Perciavalle V, Berretta S, Raffaele R. Projections from the intracerebellar nuclei to the ventral midbrain tegmentum in the rat. Neuroscience. 1989; 29:109–119. [PubMed: 2469037]

27. Schwarz C, Schmitz Y. Projection from the cerebellar lateral nucleus to precerebellar nuclei in the mossy fiber pathway is glutamatergic: A study combining anterograde tracing with immunogold labeling in the rat. J Comp Neurol. 1997; 381:320–34. [PubMed: 9133571]

28. Snider RS, Maiti A, Snider SR. Cerebellar pathways to ventral midbrain and nigra. Experimental Neurology. 1976; 53:714–728. [PubMed: 1001395]

29. Del Arco A, Mora F. Glutamate-dopamine in vivo interaction in the prefrontal cortex modulates the release of dopamine and acetylcholine in the nucleus accumbens of the awake rat. Journal of Neural Transmission. 2005; 112:97–109. [PubMed: 15599608]

30. Middleton FA, Strick PL. Cerebellar projections to the prefrontal cortex of the primate. Journal of Neuroscience. 2001; 21:700–712. [PubMed: 11160449]

31. Pinto A, Jankowski M, Sesack SR. Projections from the paraventricular nucleus of the thalamus to the rat prefrontal cortex and nucleus accumbens shell: Ultrastructural characteristics and spatial relationships with dopamine afferents. The Journal of Comparitive Neurology. 2003; 459:142–155.

32. Rogers TD, Dickson PE, Heck DH, Goldowitz D, Mittleman G, Blaha CD. Connecting the dots of the cerebro-cerebellar role in cognitive function: Neuronal pathways for cerebellar modulation of dopamine release in the prefrontal cortex. Synapse. 2011; 65:1204–1212. [PubMed: 21638338]

33. Goodrich-Hunsaker NJ, Wong LM, McLennan Y, Tassone F, Harvey D, Rivera SM, Simon TJ. Adult female fragile X permutation carriers exhibit age- and CGG repeat length-related impairments on an attentionally based enumeration task. Front Hum Neurosci. 2011; 5:63. [PubMed: 21808616]

34. Verkerk AJ, Pieretti M, Sutcliffe JS, Fu YH, Kuhl DP, Pizzuti A, Warren ST. Identification of a gene (FMR-1) containing a CGG repeat coincident with a breakpoint cluster region exhibiting length variation in fragile X syndrome. Cell. 1991; 65:905–914. [PubMed: 1710175]

35. Ellegood J, Pacey LK, Hampson DR, Lerch JP, Henkelman RM. Anatomical phenotyping in a mouse model of Fragile X syndrome with magnetic resonance imaging. Neuroimage. 2010; 53:1023–1029. [PubMed: 20304074]

36. Koekkoek SK, Yamaguchi K, Milojkovic BA, Dortland BR, Ruigrok TJ, Maex R, De Zeeuw CI. Deletion of Fmr1 in Purkinje cells enhances parallel fiber LTD, enlarges spines, and attenuates cerebellar eyelid conditioning in Fragile X syndrome. Neuron. 2005; 47:339–352. [PubMed: 16055059]

37. Paxinos, G.; Franklin, KBJ. The Mouse Brain in Stereotaxic Coordinates. 2nd. San Diego, CA: Academic Press; 2001.

38. Linnemann C, Sultan F, Pedroarena CM, Schwarz C, Thier P. Lurcher mice exhibit potentiation of GABA(A)-receptor-mediated conductance in cerebellar nuclei neurons in close temporal relationship to Purkinje cell death. J Neurophysiol. 2004; 91:1102–7. [PubMed: 14534284]

39. The Dutch-Belgian Fragile X Consortium. Fmr1 knockout mice: a model to study fragile X mental retardation. Cell. 1994; 78:23–33. [PubMed: 8033209]

40. Kooy RF, D'Hooge R, Reyniers E, Bakker CE, Nagels G, De Boulle K, Storm K, Clincke G, De Deyn PP, Oostra BA, Willems PJ. Transgenic mouse model for the fragile X syndrome. Am J Med Genet. 1996; 64:241–245. [PubMed: 8844056]

41. D'Hooge R, Nagels G, Franck F, Bakker CE, Reyniers E, Storm K, Kooy RF, Oostra BA, Willems PJ, De Deyn PP. Mildly impaired water maze performance in male Fmr1 knockout mice. Neuroscience. 1997; 76:367–76. [PubMed: 9015322]

42. Bontekoe CJ, McIlwain KL, Nieuwenhuizen IM, Yuva-Paylor LA, Nellis A, Willemsen R, et al. Knockout mouse model for Fxr2: a model for mental retardation. Hum Mol Genet. 2002; 11:487–98. [PubMed: 11875043]

43. Greco CM, Navarro CS, Hunsaker MR, Maezawa I, Shuler JF, Tassone F, Hagerman RJ. Neuropathologic features in the hippocampus and cerebellum of three older men with fragile X syndrome. Molecular Autism. 2011; 2:2. [PubMed: 21303513]

44. Sabaratnam M. Pathological and neuropathological findings in two males with fragile-X syndrome. Journal of Intellectual Disability. 2000; 44:81–85.

45. Hallahan B, Daly EM, McAlonan G, Loth E, Toal F, O'Brien F, Murphy DG. Brain morphometry volume in autistic spectrum disorder: A magnetic resonance imaging study of adults. Psychological Medicine. 2009; 39:337–346. [PubMed: 18775096]

46. McKelvey JR, Lambert R, Mottron L, Shevell MI. Right-hemisphere dysfunction in Asperger's syndrome. Journal of Child Neurology. 1995; 10:310–314. [PubMed: 7594267]

47. Yu KK, Cheung C, Chua SE, McAlonan GM. Can Asperger syndrome be distinguished from autism? An anatomic likelihood meta-analysis of MRI studies. Journal of Psychiatry and Neuroscience. 2011; 36:412–421. [PubMed: 21406158]

48. Murakami JW, Courchesne E, Haas RH, Press GA, Yeung-Courchesne R. Cerebellar and cerebral abnormalities in Rett syndrome: A quantitative MR analysis. American Journal of Roentgenology. 1992; 159:177–183. [PubMed: 1609693]

49. Oldfors A, Sourander P, Armstrong DL, Percy AK, Witt-Engerström I, Hagberg BA. Rett syndrome: cerebellar pathology. Pediatric Neurology. 1990; 6:310–314. [PubMed: 2242172]

50. Carper RA, Courchesne E. Localized enlargement of the frontal lobe in autism. Biological Psychiatry. 2005; 57:126–133. [PubMed: 15652870]

51. Kumar A, Sundaram SK, Sivaswamy L, Behen ME, Makki MI, Ager J, Chugani DC. Alterations in frontal lobe tracts and corpus callosum in young children with autism spectrum disorder. Cerebral Cortex. 2010; 20:2103–2113. [PubMed: 20019145]

52. Carper RA, Courchesne E. Inverse correlation between frontal lobe and cerebellum sizes in children with autism. Brain. 2000; 123:836–844. [PubMed: 10734014]

53. Hardan AY, Girgus RR, Adams J, Gilbert AR, Keshaven MS, Minshew NJ. Abnormal brain size effect on the thalamus in autism. Psychiatry Research: Neuroimaging. 2006; 147:145–151.

54. Tamura R, Kitamura H, Endo T, Hasegawa N, Someya T. Reduced thalamic volume observed across different subgroups of autism spectrum disorders. Psychiatry Research: Neuroimaging. 2010; 184:186–188.

55. Tsatsanis KD, Rourke BP, Klin A, Colkmar FR, Cicchetti D, Schultz RT. Reduced thalamic volume in high-functioning individuals with autism. Biological Psychiatry. 2003; 53:121–129. [PubMed: 12547467]

56. Estes A, Shaw DW, Sparks BF, Friedman S, Giedd JN, Dawson G, Dager SR. Basal ganglia morphometry and repetitive behavior in young children with autism spectrum disorder. Autism Research. 2011; 4:212–220. [PubMed: 21480545]

57. Ernst M, Zametkin AJ, Matochik JA, Pascualvaca D, Cohen RM. Low medial prefrontal dopaminergic activity in autistic children. Lancet. 1997; 350:638. [PubMed: 9288051]

58. Aalto S, Brüch A, Laine M, Rinne J. Frontal and temporal dopamine release during working memory and attention tasks in healthy humans: A positron emission tomography study using the high-affinity dopamine D2 receptor ligand [11C]FLB 457. J Neuroscience. 2005; 25:2471–2477.

59. Gamo NJ, Wang M, Arnsten AF. Methylphenidate and atomoxetine enhance prefrontal function through α2-adrenergic and dopamine D1 receptors. Journal of the American Academy of Child and Adolescent Psychiatry. 2010; 49:1011–1023. [PubMed: 20855046]

60. Jackson ME, Moghaddam B. Stimulus-specific plasticity of prefrontal cortex dopamine neurotransmission. Journal of Neurochemistry. 2004; 88:1327–1334. [PubMed: 15009632]

61. Rose J, Schiffer AM, Dittrich L, Güntürkün O. The roles of dopamine in maintenance and distractibility of attention in the "prefrontal cortex" of pigeons. Neuroscience. 2010; 167:232–237. [PubMed: 20149845]

62. Reader TA, Strazielle C, Botez MI, Lalonde R. Brain dopamine and amino acid concentrations in Lurcher mutant mice. Brain Research Bulletin. 1998; 15:489–493. [PubMed: 9570718]

63. Strazielle C, Lalonde R, Amdiss F, Botez MI, Hébert C, Reader TA. Distribution of dopamine transporters in basal ganglia of cerebellar ataxic mice by [125I]RTI-121 quantitative autoradiography. Neurochemistry International. 1998; 32:61–68. [PubMed: 9460703]

64. Myslivecek J, Cendelín J, Korelusová I, Kunová M, Markvartová V, Vozeh F. Changes of dopamine receptors in mice with olivocerebellar degeneration. Prague Medical Report. 2007; 108:57–66.
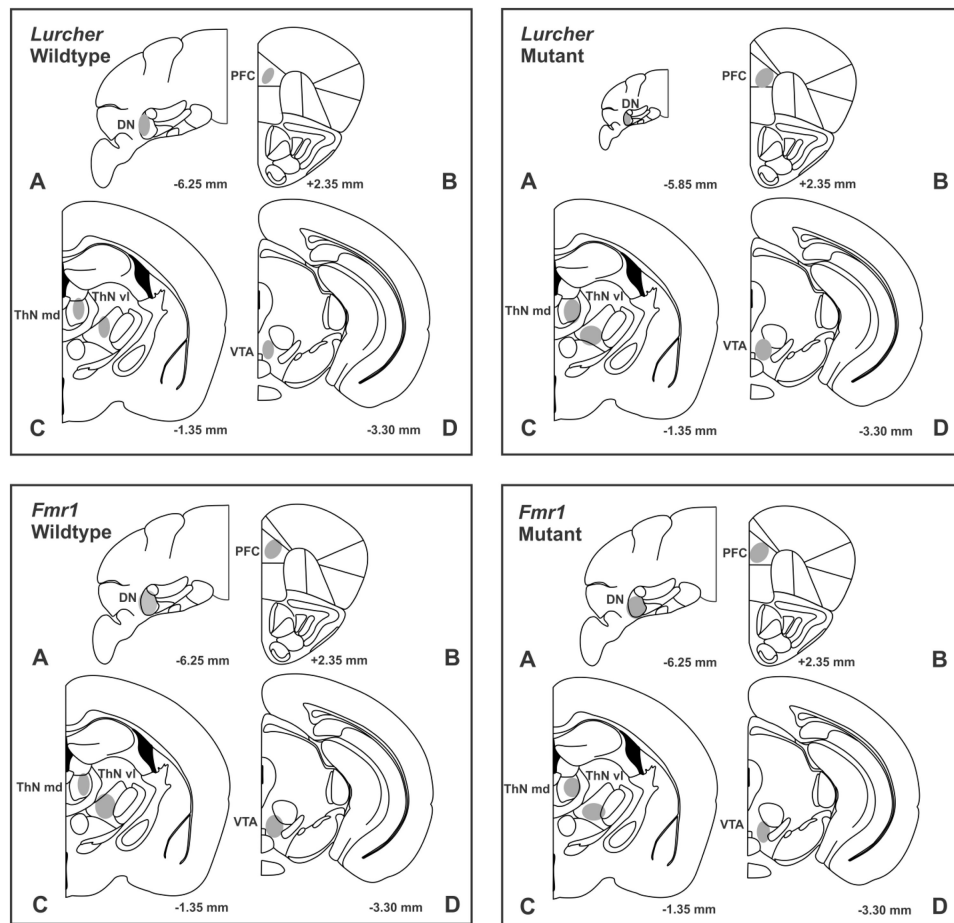
Fig. 1.
Representative coronal sections in *Lurcher* and *Fmr1* wildtype and mutant mice illustrating placements (gray shaded areas) of (A) stimulating electrodes in the dentate nucleus (DN), (B) dopamine recording electrodes in the medial prefrontal cortex (mPFC), (C) infusion cannulae in mediodorsal thalamus (ThN md) and ventrolateral thalamus (ThN vl), and (D) infusion cannulae in the ventral tegmental area (VTA). Numbers correspond to mm from bregma. Placements of stimulating and recording electrodes, and cannula placements overlapped in all groups. Sections were adapted from the mouse atlas of [37].
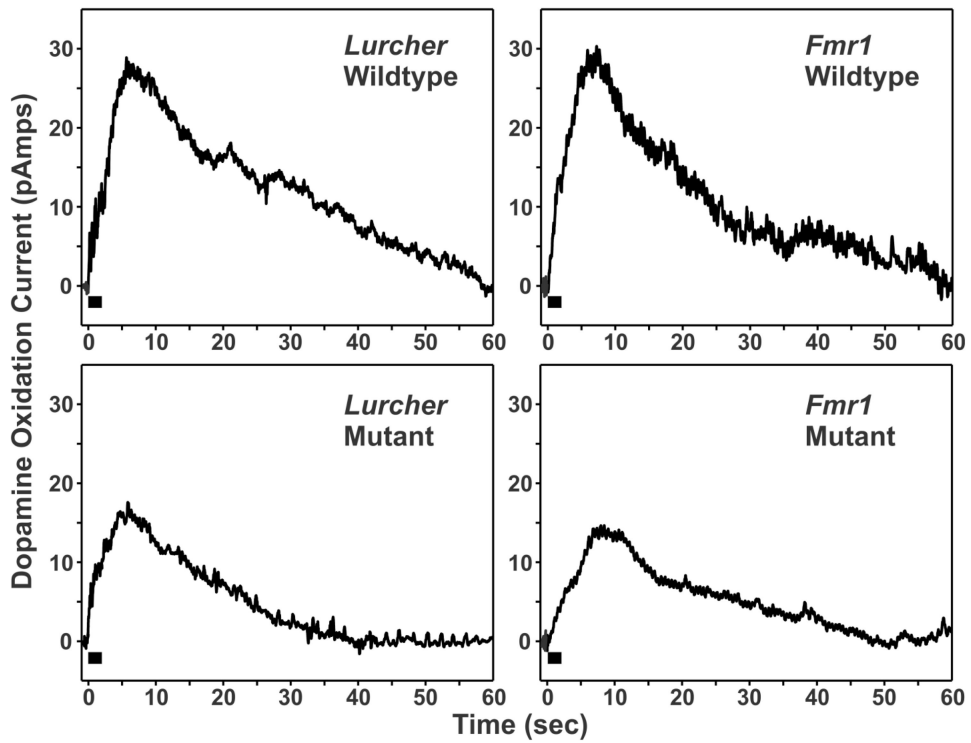
Fig. 2.
Individual examples of changes in medial prefrontal cortex (mPFC) dopamine oxidation current (corresponding to changes in extracellular dopamine concentrations) in *Lurcher* and *Fmr1* wildtype and mutant mice evoked by electrical stimulation of the cerebellar dentate nucleus (black bar, 100 pulses at 50 Hz) just prior to drug infusion. Mutant mice of both strains consistently showed a marked attenuation in the mPFC dopamine response.
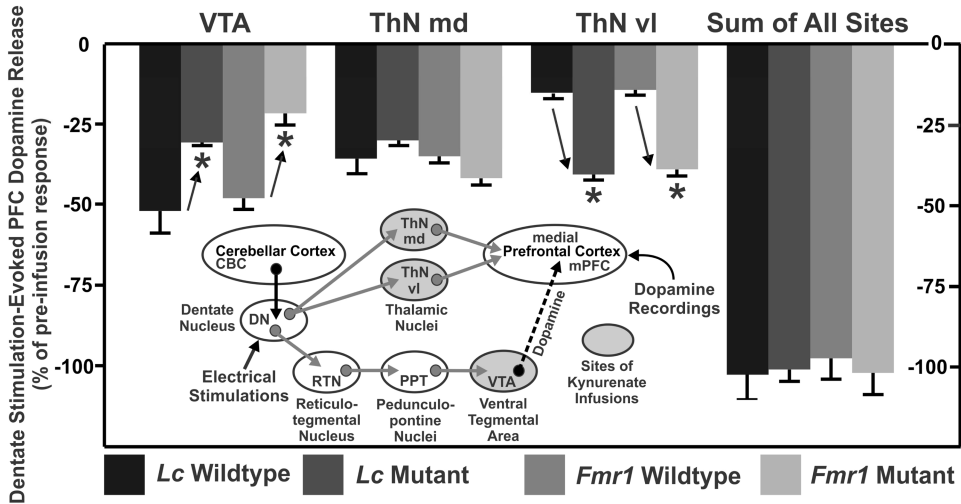
Fig. 3.
Average percent decrease in dentate nucleus (DN) stimulation-evoked dopamine responses following kynurenate infusion into the ventral tegmental area (VTA), mediodorsal thalamus (ThN md), or the ventrolateral thalamus (ThN vl), as well as the summed average percent decrease of each drug infused across sites. In *Lurcher* and *Fmr1* wildtype mice infusions of kynurenate into the VTA reduced dopamine responses by ~50%, while kynurenate infusions into the thalamus (md and vl combined) also reduced the dopamine response by a total of ~50% (md = ~35% and vl = ~15%). In contrast, the reduction in the dopamine response following kynurenate into the VTA in *Lurcher* mutant (~30%) and *Fmr1* mutant (~20%) mice was significantly less, indicating a reduction in the modulatory strength of this pathway. This reduction in strength in mutant mice was coupled to an increase in signal strength of the pathway through the thalamus, specifically the ThN vl. Thus, kynurenate infused into this nucleus reduced dopamine responses by ~15 % in wildtype mice of both strains and ~40% in mutant mice of both strains. Regardless of strain or genotype kynurenate infused into the ThN md reduced the dopamine signal between 30 to 40%. The inset figure shows the two independent pathways by which cerebellar output through the DN modulates dopamine release in the mPFC. See text for additional description.

Table 1

Infusion site-specific percent decrease (±S.E.M.) of mPFC dopamine release following intra-VTA, ThN md, or ThN vl infusions of PBS (top), lidocaine (middle), or kynurenate (bottom) in *Lurcher* and *Fmr1* wildtype and mutant mice.

Drug Infused	Site of Infusion	Mouse Strain and Genotype			
		Lurcher Wildtype n=45	*Lurcher* Mutant n=54	*Fmr1* Wildtype n=45	*Fmr1* Mutant n=45
PBS	VTA	2.8 % ± 1.3 %	1.0 % ± 0.9 %	2.4 % ± 0.9 %	0.8 % ± 0.8 %
	ThNmd	2.0 % ± 1.1 %	2.8 % ± 0.8 %	1.3 % ± 0.8 %	2.4 % ± 0.9 %
	ThNvl	0.8 % ± 1.3 %	1.4 % ± 1.3 %	0.1 % ± 0.4 %	0.4 % ± 0.8 %
Lidocaine	VTA	51.8 % ± 11.3 %	29.3 % ± 2.2 %	47.9 % ± 3.4 %	21.5 % ± 3.3 %
	ThNmd	35.6 % ± 4.4 %	31.1 % ± 0.7 %	35.3 % ± 1.5 %	41.6 % ± 1.6 %
	ThNvl	15.2 % ± 2.4 %	40.8 % ± 2.9 %	14.3 % ± 1.0 %	38.9 % ± 1.3 %
Kynurenate	VTA	49.23% ± 6.2 %	29.9 % ± 1.7 %	48.8 % ± 1.3 %	19.6 % ± 1.2 %
	ThNmd	35.4 % ± 4.4 %	30.3 % ± 1.4 %	35.2 % ± 1.7 %	40.4 % ± 3.4 %
	ThNvl	15.3 % ± 2.4 %	38.8 % ± 1.9 %	14.9 % ± 0.5 %	40.7 % ± 1.4 %